AJNR

MR of carcinoma-specific monoclonal antibody conjugated to monocrystalline iron oxide nanoparticles: the potential for noninvasive diagnosis.

L G Remsen, C I McCormick, S Roman-Goldstein, G Nilaver, R Weissleder, A Bogdanov, I Hellström, R A Kroll and E A Neuwelt

AJNR Am J Neuroradiol 1996, 17 (3) 411-418
http://www.ajnr.org/content/17/3/411

MR of Carcinoma-Specific Monoclonal Antibody Conjugated to Monocrystalline Iron Oxide Nanoparticles: The Potential for Noninvasive Diagnosis

Laura G. Remsen, Christopher I. McCormick, Simon Roman-Goldstein, Gajanan Nilaver, Ralph Weissleder, Alexei Bogdanov, Karl E. Hellström, Ingegerd Hellström, Robert A. Kroll, and Edward A. Neuwelt

PURPOSE: To determine if tumor-specific monoclonal antibodies conjugated to superparamagnetic monocrystalline iron oxide nanoparticles can be used to yield specific diagnoses with the use of MR imaging. **METHODS:** Monoclonal antibodies conjugated to monocrystalline iron oxide nanoparticles were given to nude rats with intracranial tumors either by intravenous injection, intraarterial injection with osmotic blood-brain barrier disruption, or direct intratumoral inoculation. Either L6, a tumor-specific antibody, or P-1.17, a control isotype-matched antibody, was used. Coronal T1-weighted, T2-weighted, and spoiled gradient-recalled acquisition in the steady state images were obtained before, 30 minutes after, 6 hours after, and 24 hours after injection. **RESULTS:** Intravenous injection of greater than 2 mg of the tumor-specific antibody showed a specific pattern of enhancement of the tumors with the largest concentration of antibody in the area with the greatest density of tumor cells. The control antibody showed nonspecific changes. After intraarterial injection with barrier disruption to increase delivery globally or direct inoculation to increase delivery focally, no specific enhancement pattern was seen. **CONCLUSION:** Monoclonal antibodies conjugated with monocrystalline iron oxide particles may provide a method to obtain specific diagnoses with the use of MR imaging.

Index terms: Antigens and antibodies; Brain neoplasms, magnetic resonance; Carcinoma; Animal studies

AJNR Am J Neuroradiol 17:411–418, March 1996

One of the limitations of neuroimaging of brain tumors is that no technique has been able to give a definitive pathologic diagnosis or to determine accurately the extent of an intracranial lesion (1). Current techniques show mass effects, contrast enhancement, and altered signal intensity in brain tumors. Enhancement is usually caused by blood-brain barrier (BBB) compromise and neovascularity, whereas altered signal is usually the result of increased water content. Paramagnetic or superparamagnetic substances conjugated to tumor-specific monoclonal antibodies may have the potential to identify specifically tumor type and its extent in the brain.

Paramagnetic gadolinium chelates have been used clinically as magnetic resonance (MR) imaging agents to evaluate areas of BBB compromise; however, the conjugation of adequate amounts of gadolinium to tumor-specific monoclonal antibodies is difficult to achieve. The use of diethylenetriamine pentaacetic acid (DTPA) as a chelating agent results in a maximum of 4 to 20 gadolinium molecules per antibody molecule (2). Because of the low number of gadolinium molecules and relatively low magnetic susceptibility, it is necessary to deliver concen-

Received May 4, 1995; accepted after revision September 18.

Supported by the Veterans Administration Merit Review grant and the National Institutes of Health grants CA59649, NS27757, and CA59649–01.

From the Departments of Neurology (L.G.R., R.A.K., E.A.N.), Biochemistry and Molecular Biology (E.A.N.), Radiology (S.R.G.), Cell Biology and Anatomy (G.N.), and Ophthalmology (G.N.), Oregon Health Sciences University, Portland; VA Medical Center, Portland, Ore (C.I.M.); Department of Radiology, Massachusetts General Hospital-NMR Center, Harvard Medical School, Boston (R.W., A.B.); and Bristol-Myers Squibb, Pharmaceutical Research Institute, Seattle, Wash (K.E.H., I.H.).

Address reprint requests to Edward A. Neuwelt, MD, Oregon Health Sciences University, Department of Neurology (L603), 3181 SW Sam Jackson Park Rd, Portland, OR 97201.

AJNR 17:411–418, Mar 1996 0195-6108/96/1703–0411

trations in the range of 10^{-4} mol/L of the paramagnetic label to the target tissue. This is considerably higher than the amount necessary for radionuclide imaging, which only requires carrier concentrations in the range of 10^{-11} mol/L (Göhr-Rosenthal S, Schmitt-Willich H, Ebert W, et al, "An Immunoselective Contrast Medium for MRI: Detection of Colorectal Tumor Transplants in Mice with a Gadolinium-Labeled Monoclonal Antibody," *Radiol Res* 1993;1:356, abstract).

This study was undertaken to determine whether a monoclonal antibody conjugated to monocrystalline iron oxide nanoparticles (MION) retained antigenic specificity both in vitro and in vivo in a rodent model of a human small-cell lung carcinoma xenograft and whether MION conjugated to a tumor-specific monoclonal antibody would result in different enhancement patterns from those of unconjugated MION or MION conjugated to a control (nonspecific) antibody. Last, experiments were done to determine whether intravenous injection, intracarotid injection with osmotic BBB disruption, or direct inoculation into the brain would be the best route of delivery for tumor-specific imaging of MION-conjugated monoclonal antibodies (antibody-MION).

Materials and Methods

Monoclonal Antibodies

L6 is a mouse monoclonal IgG_{2a} antibody reactive with a propressophysin-like protein cell surface antigen abundant on human small-cell lung carcinoma, breast carcinoma, and colon carcinoma (3, 4). P1.17, used as the control IgG_{2a} antibody, is reactive against mouse myeloma protein. These antibodies were provided by Bristol-Myers Squibb Pharmaceutical Research Institute (Seattle, Wash). L6 and P1.17 monoclonal antibodies have been well characterized both in vitro and in vivo by immunohistochemistry and Scatchard analysis (4). Membrane extracts from LX-1 cells and the propressophysin-like antigen extract have been studied by Western blot analysis. These studies have shown immunoreactivity of L6 IgG and the lack of immunoreactivity of P1.17 (3–6).

Antibody-MION Preparation

To conjugate the antibody to MION, we first incubated MION with $NaIO_4$ [initial dextran/$NaIO_4$ ratio = 1:1 (wt/wt) MION/L6 ratio (mg) = 1:2] in 0.01 mol/L citrate buffer, pH 8.4, at room temperature and then purified it on a Sephadex G-100 column. The product of this reaction was then conjugated to the monoclonal antibodies (L6 or P1.17) in a 0.2 mmol/L sodium bicarbonate buffer, pH 6.5 for 15 minutes at room temperature. Subsequently, 10 mg of $NaCNBH_3$ was added to reduce the Schiff base. Ultimately, purification was performed by ultrafiltration (Amicon filter) followed by gel chromatography on a Biogel A15 column to separate free from bound antibody. Typically, approximately 12 monoclonal antibodies were bound per MION colloid. The antibody-MION conjugates and MION were provided by the MR Pharmaceutical Program of Massachusetts General Hospital (Boston, Mass).

Tumor Cell Growth and Inoculation

LX-1 tumor cells were maintained in culture as previously described (7). Adult female nude rats from the National Institutes of Health breeding colony were stereotaxically inoculated in the right caudate-putamen as described previously (8–10).

In Vitro Cell Binding Assay

Immunoreactivity of the antibody-MION conjugates was evaluated before each use by a cell binding assay. One hundred micrograms of L6, L6-MION, P1.17, and P1.17-MION were iodinated by the Iodo-gen method (Pierce, Rockford, Ill). The specific activities of these compounds were approximately equal, and they measured between 2.29 and 2.97 μCi/μg. The assay was then performed in duplicate as follows: (*a*) 5×10^6 LX-1 cells were placed into a 12 × 75-mm tube; (*b*) 1 ng of iodinated monoclonal antibody or antibody-MION (10 000 cpm) was added to each tube; (*c*) the tubes were allowed to incubate at room temperature for 30 minutes, with agitation every 5 minutes; (*d*) after the incubation period, 1.25 mL of phosphate buffered saline was added to each of the tubes, which were then centrifuged; and (*e*) the pellet and supernatant from each tube were then separated and counted on a gamma counter. Cell binding was calculated from the following formula: cell binding = [pellet/(pellet + supernatant)] × 100.

Iron Delivery

All rats were treated 9 days after tumor cell inoculation. MR images were evaluated subjectively in comparison with noncontrast images by three of the authors of this article as well as by an external blinded reviewer.

Intravenous administration.—Antibody-MION or MION alone as a control agent was administered to rats at an iron dose of 5–10 mg/kg as an intravenous bolus injection. MR images were obtained 30 minutes (n = 11), 6 hours (n = 9), and 24 hours (n = 3) after treatment.

BBB disruption.—Osmotic disruption of the BBB in the right (tumor-bearing) hemisphere was done as previously described (7, 11). Briefly, rats were anesthetized with pentobarbital sodium and a catheter filled with heparinized saline was tied into the right external carotid artery for retrograde infusion of mannitol, followed by antibody-MION or MION alone. Each animal received a dose of 5 to 10 mg/kg of iron and then underwent MR imaging 30 minutes (n = 7), 6 hours (n = 8), and 24 hours (n = 10)

after treatment. The use of BBB disruption to increase delivery of chemotherapeutic agents to the brain has clinical and laboratory applicability (12, 13). It increases the delivery of monoclonal antibodies to the brain tumor, the brain around the tumor, and the ipsilateral normal area of the brain (11, 14).

Focal inoculation.—Antibody-MION or MION alone was administered to rats by direct inoculation into the intracerebral tumor as previously described (7). Clinically, application of high-flow microinfusion directly into the brain has been shown to cause significant tumor regression (Laske DW, Youle RJ, Ilercil O, et al, "Clinical Experience with Convection-Enhanced Drug Delivery in the Brain," *Neurosurgery* 1994;35:576, abstract). Each animal received a 5-μg dose of iron (which is approximately equivalent to the intracerebral delivery after an intracarotid dose of 10 mg/kg of iron given immediately after osmotic BBB disruption) and then had MR imaging 30 hours (n = 9) and 100 hours (n = 9) after treatment.

Imaging Protocols

We used a 1.5-T Signa MR unit (General Electric, Milwaukee, Wis) with a receive-only loop-gap resonator coil specifically engineered for rodent imaging. Coronal T1-weighted images were obtained with 300/16/4 (repetition time/echo time/excitations), a 256 × 192 matrix, a 9-cm field of view, and a 3-mm section thickness. Coronal T2-weighted images were obtained with a fast spin-echo technique with parameters of 3000/116/1, a 256 × 192 matrix, a 9-cm field of view, and a 3-mm section thickness. Coronal spoiled gradient-echo (SPGR) images were obtained with parameters of 60/9/2, a flip angle of 45°, a 256 × 192 matrix, a 9-cm field of view, and 0.7-mm section thickness.

Image Analysis

Similar to the method described by Kelly et al (15), our method correlates MION enhancement characteristics to tumor region. As reported, tumors were divided into a central zone of necrosis and/or cyst (zone 1), an enhancing ring of dense tumor (zone 2), and a peripheral zone of infiltrating tumor cells (zone 3). A three-ring sign was postulated by combining the signal changes resulting from increasing concentrations of iron given by the Solomon-Bloembergen equations and by the fact that, according to the work of Kelly et al, the greatest tumor cell density and thus the greatest iron concentration would be in zone 2, with lower concentrations in zones 1 and 3. Any other pattern of enhancement was called amorphous. Cyst size was measured visually as none, small,or large. Tumor size, which corresponded to the rim of enhancement (zone 2) in the study by Kelly et al (15), was graded visually as none, 0; small, 1; or large, 2.

Histochemical Staining for Iron

Rats were killed immediately after MR imaging by barbiturate overdose. Following intravenous administration or direct inoculation, their brains were immersion-fixed in 10% neutral buffered formalin for histochemical analyses. After iron delivery by BBB disruption, the brains were perfusion-fixed. Each brain was blocked and then sectioned at 100 μm in the coronal plane by means of a Vibratome. Iron was detected histologically via a modification of the Prussian blue staining method with diaminobenzidine intensification, as described previously (7).

Results

Antigen Specificity of Immunoconjugates

Cell binding assays revealed in vitro reactivity of L6 and P1.17 antibody-MION conjugates with LX-1 cells. The results of the cell binding assay at 1 ng monoclonal antibody per 5×10^6 cells for the L6, P1.17, L6-MION, and P1.17-MION are as follows: The percentage of binding of L6 to LX-1 cells ranged from 60% to 90%. The isotype-matched control P1.17 had a cell binding of 3% to 5%. A modest decrement in cell binding occurred when MION was conjugated to the L6 or P1.17 monoclonal antibodies (10% to 20% of total cell binding).

Tumor-Specific Location after Intravenous Administration

Initially, at 30 minutes, L6-MION (n = 11) resulted in no signal change relative to the baseline scan; however, at 6 hours (n = 9), images showed markedly better enhancement when compared with P1.17-MION (n = 10), the control antibody. The tumors appeared hypointense relative to brain on T1-weighted images obtained before administration of immunoconjugate (Figs 1A and 2A) with no change 30 minutes after delivery (Figs 1B and 2B). Six hours after administration, T1-weighted images showed a characteristic enhancement pattern (Figs 1C and 2C). With L6-MION, changes in signal were apparent in all three zones on T1-weighted images (n = 5) (Fig 1C). Zones 1 and 3 showed increased signal, and zone 2 (dense tumor) showed decreased signal. With the P1.17-MION (Fig 2C), some hyperintensity was observed in the central zone, but little change in signal intensity was seen in zones 2 or 3.

After intravenous administration of MION alone (n = 3), some amorphous enhancement was present at 6 hours, similar to that seen with

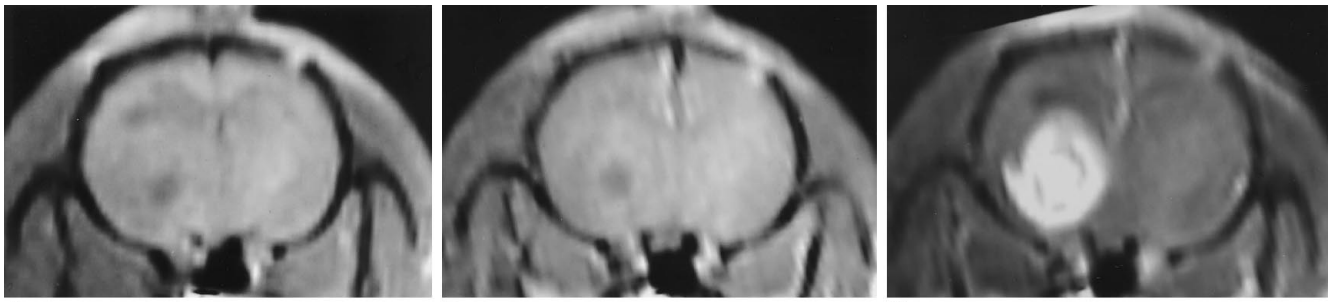

Fig 1. Coronal T1-weighted MR images obtained with parameters of 300/16/4 (repetition time/echo time/excitations) in a rat that received L6-MION (iron dose of 10 mg/kg, monoclonal antibody dose of 5.04 mg) as an intravenous bolus injection.

A, MR image before injection of monoclonal antibody-MION shows a large tumor in the right cerebral hemisphere.

B, MR image 30 minutes after intravenous infusion shows no appreciable change in signal.

C, MR image 6 hours after intravenous infusion shows a characteristic enhancement pattern consisting of three zones. These can best be described as a central area of hyperintensity (zone 1), surrounded by an area of hypointensity corresponding to dense tumor (zone 2), and a peripheral rim of hyperintensity corresponding to increased free water and infiltrating tumor (zone 3).

P1.17-MION; however, this was gone at 24 hours. On T2-weighted images obtained after administration of L6-MION, the only change observed was hypointensity in zone 2, the ring of highest cell density and immunoconjugate binding. The SPGR images showed a similar pattern to the T1-weighted images. When the sections were stained immunochemically for the presence of antibody, none was detected. Immediate neurotoxicity (ie, seizures) due to the MIONs or antibody-MIONs was not observed.

MION Imaging after Delivery by BBB Disruption

When the immunoconjugates were delivered via the carotid artery with BBB disruption (n = 15), in contrast to intravenous administration, changes in signal intensity were seen immediately afterward. These changes appeared as increased signal intensity throughout the disrupted hemisphere, caused by increased delivery to the entire hemisphere, and they were still apparent 6 hours after BBB disruption (Fig 3A and B). With increased signal intensity in the entire hemisphere seen with BBB disruption, changes associated with delivery to tumor were not clear. With intracarotid delivery after BBB disruption, signal enhancement was still present at 24 hours but was no longer seen when the animal was killed at 100 hours. With intravenous delivery after BBB disruption, signal changes were no longer visible at 24 hours. Examination of hematoxylin-eosin stained sections often revealed the presence of a central area of necrosis and cystic degeneration (Fig 3C). Adjacent sections stained for iron (Fig 3D)

Fig 2. Coronal T1-weighted MR images obtained with parameters of 300/16/4 in a rat that received P1.17-MION (iron dose of 10 mg/kg, monoclonal antibodies dose of 5.61 mg) as an intravenous bolus injection.

A, MR image before monoclonal antibody-MION injection shows a large tumor with a large cyst in the right cerebral hemisphere.

B, MR image 30 minutes after intravenous infusion shows no appreciable change.

C, MR image 6 hours after intravenous infusion shows hyperintensity in zone 1 and little change in zones 2 or 3.

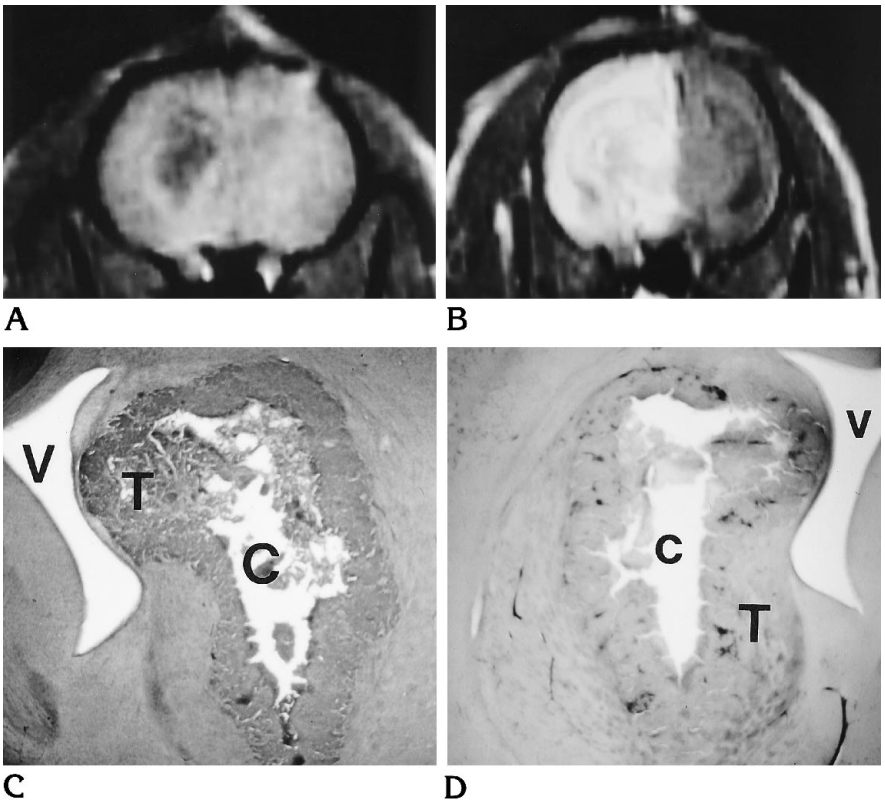

Fig 3. *A* and *B*, Coronal T1-weighted images obtained with parameters of 300/16/4 in a rat that received P1.17-MION (10 mg/kg iron dose, antibody dose of 2.07 mg) to the brain by BBB disruption.

A, MR image before monoclonal antibody-MION injection shows a large tumor with a large hypointense cyst in the right cerebral hemisphere.

B, MR image acquired 6 hours after BBB disruption shows increased signal enhancement diffusely throughout the right cerebral hemisphere.

C, Histologic section of the right cerebral hemisphere shows the large necrotic cystic area in the center of the tumor corresponding to the area of hypointensity seen in *A*. *V* = ventricle, *C* = cyst, *T* = tumor. (Hematoxylin-eosin stain.)

D, Histologic section of the immediately adjacent section shows minimal patchy staining of tumor cells and a small amount of iron staining in brain around tumor. *V* = ventricle, *C* = cyst, *T* = tumor. (Prussian blue stain.)

showed that only a small amount of iron was taken up into very few tumor cells as well as minimally into surrounding normal brain.

Delivery by Focal Inoculation

The immunoconjugates were also administered by direct inoculation into the tumor site (n = 9). MR images acquired 100 hours after treatment showed an amorphous area of hyperintensity evident in the area of the tumor, and histologic analyses of sections stained for iron showed minimal patchy staining within the tumor and a small amount of uptake in the brain around the tumor.

Statistical Analysis

Statistical analyses were limited to those animals that received intravenous administration. Cyst size did not correlate with the appearance of the three-ring enhancement, nor did the tumor size. There was a significant difference in MR images when the dose of antibody administered was greater than 2 mg ($P = .0476$, Table). In those animals receiving the higher dose of tumor-specific L6-MION, the three-ring enhancement was seen in four of four animals. Of those animals receiving less than 2 mg of antibody, the three-ring enhancement was seen only in one of five animals. This was not true for control P1.17-MION. A three-ring enhancement was seen in one animal who received P1.17-MION; this animal received an antibody dose of 0.73 mg.

Discussion

The evaluation of enhancing lesions presents a problem in diagnosis and in assessment of tumor extent. Even in patients with a known primary neoplasm, intracranial lesions thought to be metastases turn out to be a different disease 11% of the time (16, 17). Prior results with antibodies and gadopentetate dimeglumine have shown increased specificity, but large amounts of gadolinium are necessary for MR visualization (Göhr-Rosenthal S et al, "An Immunoselective...").

Until recently, use of superparamagnetic magnetite particles attached to antibody has been of limited value. The large size of these reported particles (50 to 2000 nm) resulted in their rapid clearance from the blood by liver and

MR findings 6 hours after intravenous delivery of immunoconjugate: correlation of antibody dose with significant enhancement

Treatment	Rat	Antibody Dose, mg	Tumor Size	Cyst Size	T1 Enhancement
L6-MION					
	887	2.40	1	Large	Three-ring effect*
	891	5.60	2	Large	Three-ring effect*
	892	5.04	2	Small	Three-ring effect*
	915	1.78	1	Small	Amorphous
	920	0.53	2	Large	Amorphous
	921	0.40	2	Large	Amorphous
	923	1.44	2	Large	Three-ring effect*
	924	1.16	2	Large	Amorphous
	980	3.98	2	Large	Three-ring effect*
P1.17-MION control antibody					
	889	5.61	2	Large	Amorphous
	890	5.51	2	Large	Amorphous
	897	2.31	1	Small	Amorphous
	913	2.46	2	Large	Amorphous
	919	0.20	1	None	None
	922	0.42	1	Small	None
	925	1.41	2	Large	Amorphous
	926	1.41	2	Large	Amorphous
	979	0.73	2	Large	Three-ring effect
	982	0.69	1	None	None
MION only					
	898	0	2	Small	Amorphous
	981	0	2	Small	Amorphous
	984	0	1	Small	None

* Significant relationship between dose of monoclonal antibodies delivered with the appearance of the characteristic signal intensity changes ($P = .0476$; Fisher's Exact Test).

spleen before they could bind to antigen (18). After intravenous injection, these large particles become rapidly sequestered by the reticuloendothelial system (19). A significant advance in the use of superparamagnetic particles for MR imaging occurred when the development of ultrasmall iron oxide compounds (18) or MION (20) was reported. These MIONs can pass through capillary fenestrae and loose interendothelial junctions or vesicles to reach the interstitial space. This is valuable for MR imaging agents, because the more specific the accumulation of a contrast agent within the target tissue without distribution to surrounding tissue, the better the resulting lesion-tissue contrast (21–24).

The core of these particles is a single iron oxide crystal held within a stable dextran coat that isolates it from surrounding solutions and lowers protein adsorption to the particle surface. The MIONs remain excluded from the brain by the normal BBB; however, we have demonstrated that these MIONs can be delivered across the BBB with osmotic BBB disruption and can be shown with MR imaging in the brains of rats at doses as low as 1 μg (7). The MION relaxivities (measured in aqueous solution at 37°C) for R1 and R2 are 16.5 $(\text{mmol}\cdot\text{s})^{-1}$, and 34.8 $(\text{mmol}\cdot\text{s})^{-1}$, respectively (Shibata T, Weissleder R, Schaffer B, Shen T, Papisov M, Brady TJ, "Tissue Relaxivities and Detectability of Monocrystalline Iron Oxides," presented at the annual meeting of the Society of Magnetic Resonance in Medicine, Berlin, 1993). These values are higher than the R1 and R2 for gadopentetate dimeglumine, which are 4.5 $(\text{mmol}\cdot\text{s})^{-1}$ and 5.7 $(\text{mmol}\cdot\text{s})^{-1}$, respectively (Shibata T et al, "Tissue Relaxivities..."). A lower concentration of MION is therefore needed to be detectable by MR imaging.

Intravenous Administration of MION Conjugate

A consistent enhancement pattern of three zones appeared on T1-weighted images. These three zones are best described by the scheme devised by Kelly et al (15), as outlined in "Methods." Zone 1 (central necrosis) and zone 3 (edema with peripheral infiltrating tumor) have a lower density of tumor cells and thus a lower iron concentration. Therefore, these areas were hyperintense on T1-weighted images after intravenous administration of MION. Zone 2, the ring of highest tumor density, became hypointense owing to increased iron concentration. Zones 1 and 3 were markedly hyperintense on T2-weighted images before administration of antibody-MION, and no change could be noticed after antibody-MION was administered. Zone 2 was not as hyperintense on T2-weighted images before administration of antibody-MION, because in the areas of greatest tumor cell density there is less free water, and increased free water is the major component of hyperintensity on T2-weighted images. After injection of antibody-MION, zone 2 became hypointense relative to its preinjection intensity owing to the proposed increase in antibody-MION bound by the tumor. The SPGR images showed a similar pattern to that of the T1-weighted images. Histologic evaluation of the brains of animals receiving intravenous antibody-MION showed staining in a few individual tumor cells and a modest uptake of iron into the brain around the tumor or into the normal area of the brain. When the sections were stained immunochemically for the presence of antibody, none was detected. We were unable to confirm good intracerebral localization of the L6-MION conjugates on histologic sections with Prussian blue staining. Because the tissues were fixed in 10% buffered formalin, and neither L6 nor P1.17 is a modulating monoclonal antibody, it is possible that most of the antibody-MION complex was removed in processing. Nonetheless, specific imaging was clearly observable on MR images.

Delivery of Antibody-MION after Osmotic BBB Disruption

In the present study, BBB disruption with intracarotid drug delivery was used to determine if more antibody-MION delivered to tumor would improve visibility on MR images. We found, in contrast to the intravenous studies, that we could see the antibody-MION in the disrupted hemisphere 30 minutes after BBB disruption. We could not, however, see the tumors, owing to enhancement seen throughout the disrupted hemisphere on T1-weighted images. In most of the animals that were imaged at 24 hours after BBB disruption, hemispheric enhancement was still present, but the tumors were not readily defined. When the same animals were imaged at 100 hours, no enhancement of the tumor or of the hemisphere was seen. There were no apparent differences between L6-MION, P1.17-MION, and MION alone in any of these BBB disruption studies. It remains to be seen whether imaging these tumors at other time points would allow for better tumor-specific enhancement. Future studies may test the tumor-specific localization of L6-$(ab')_2$ (a divalent fragment of L6-IgG) MION immunoconjugate given with BBB disruption to avoid nonspecific binding, particularly to assess tumor extent accurately.

Intratumoral Administration of Conjugates

No specific enhancement pattern was seen at 24 hours, nor was there a difference between L6 or P1.17-MION. At 100 hours, on T1-weighted images, tumor growth was obvious but no enhancement due to iron was present; on T2-weighted images, minimal iron was still visible. Staining of individual cells in the solid tumor was found when these sections were stained for iron. There appeared to be more uptake of the MION into normal brain around the tumor; however, this was modest.

Conclusion

Although definitive diagnosis still requires tissue, we believe MION immunoconjugates are potential imaging agents for tumor-specific MR location of intracerebral tumors. In patients with enhancing lesions, the antibody-MION may provide a method to obtain histologically specific diagnoses with MR imaging.

Acknowledgments

We express our sincere appreciation to Kathryn Griffith at Oregon Health Sciences University for her technical expertise with MR imaging and to Nasseem Nossif at Massachusetts General Hospital for preparation of iron antibody conjugates.

References

1. Davis PC, Hudgins PA, Peterman SB, Hoffman JC. Diagnosis of cerebral metastases: double-dose delayed CT vs. contrast-enhanced MR imaging. *AJNR Am J Neuroradiol* 1991;12:293–300
2. Unger EC, Totty WG, Neufeld DM, et al. Magnetic resonance imaging using gadolinium labeled monoclonal antibody. *Invest Radiol* 1985;20:693–699
3. Hellström I, Beaumler PL, Hellström KE. Antitumor effects of L6, and IgG_{2a} antibody that reacts with most human carcinomas. *Proc Natl Acad Sci (USA)* 1986;83:7059–7063
4. Hellström I, Horn D, Linsley P, Brown JP, Brankovan V, Hellström KE. Monoclonal mouse antibodies raised against human lung carcinoma. *Cancer Res* 1986;46:3917–3923
5. Goodman GE, Hellström I, Brodzinsky L, et al. Phase I trial of murine monoclonal antibody L6 in breast, colon, ovarian, and lung cancer. *J Clin Oncol* 1990;8:1083–1092
6. Nilaver G, Rosenbaum LC, Hellström KE, Hellström I, Neuwelt EA. Identification of neurophysin immunoreactivity in hypothalamus by a monoclonal antibody to a carcinoma cell surface antigen. *Neuroendocrinol* 1990;51:565–571
7. Barnett PA, Roman-Goldstein S, Ramsey F, et al. Differential permeability and quantitative MR imaging of a human lung carcinoma brain xenograft in the nude rat. *Am J Pathol* 1992;146:436–449
8. Neuwelt, EA, Weissleder R, Nilaver G, et al. Delivery of virus-sized iron oxide particles to rodent CNS neurons. *Neurosurgery* 1994; 34:777–784
9. Neuwelt EA, Barnett PA, Ramsey FL, Hellström KE, McCormick CI. Dexamethasone decreases the delivery of tumor-specific monoclonal antibody to both intracerebral and subcutaneous tumor xenographs. *Neurosurgery* 1993;33:478–484
10. Roman-Goldstein SM, Barnett PA, McCormick CI, et al. Effects of Gd-DTPA after osmotic BBB disruption in a rodent model: toxicity and MR findings. *J Comput Assist Tomogr* 1994;18:731–736
11. Neuwelt EA, Barnett PA, Hellström KE, et al. Delivery of melanoma-specific immunoglobulin monoclonal antibody and Fab fragments to normal brain utilizing osmotic blood-brain barrier disruption. *Cancer Res* 1988;48:4725–4729
12. Neuwelt EA. Blood-brain barrier disruption in the treatment of brain tumors: animal studies. In: *Implications of the Blood-Brain Barrier and Its Manipulation, vol 2. Clinical Implications*. New York: Plenum Press, 1989:107–194
13. Neuwelt EA, Goldman D, Dahlborg SA, et al. Primary CNS lymphoma treated with osmotic blood-brain barrier disruption: prolonged survival and preservation of cognitive function. *J Clin Oncol* 1991;9:1580–1590
14. Neuwelt EA, Barnett PA, Hellström KE, Hellström I, McCormick CI, Ramsey FL. The effect of blood-brain barrier on intact and fragmented monoclonal antibody localization in intracerebral human carcinoma xenografts. *J Nucl Med* 1994;35:1831–1841
15. Kelly PJ, Dumas-Duport C, Kispert DB. Imaging-based stereotaxic serial biopsies in untreated intracranial glial neoplasms. *J Neurosurg* 1987;66:865–874
16. Patchell RA, Tibbs PAS, Walsh JW, et al. A randomized trial of surgery in the treatment of single metastases to the brain. *N Engl J Med* 1990;322:494–500
17. Patchell RA, Cirrincione C, Thaler HT, Galicich JH, Kim JH, Posner JB. Single brain metastases: surgery plus radiation or radiation alone. *Neurology* 1986;36:447–453
18. Weissleder R, Elizondo G, Wittenberg J, Rabito CA, Bengele HH, Josephson L. Ultrasmall superparamagnetic iron oxide: characterization of a new class of contrast agents for MR imaging. *Radiology* 1990;175:489–493
19. Weissleder R, Lee AS, Khaw BA, Shen T, Brady TJ. Antimyosin-labeled monocrystalline iron oxide allows detection of myocardial infarct: MR antibody imaging. *Radiology* 1992;182:381–385
20. Shen T, Weissleder R, Papisov M, Bogdanov A, Brady TJ. Monocrystalline iron oxide nanocompounds (MION): physicochemical properties. *Magn Reson Med* 1993;29:599–604
21. Bulte JWM, deJonge MWA, Kamman RL, Zuiderveen F, The TH, deLeij L. Magnetite as a potent contrast-enhancing agent in magnetic resonance imaging to visualize blood-brain barrier disruption. *Acta Neurochir* 1993;57:30–34
22. Haacke EM. Image behavior: resolution, signal-to-noise, contrast and artifacts. In: Modic MT, ed. *Magnetic Resonance Imaging of the Spine*. St Louis: Mosby Year Book, 1989:1–34
23. Weissleder R, Bogdanov A, Papisov M. Drug targeting in magnetic resonance imaging. *Magn Reson Imaging* 1992;8:55–63
24. Weissleder R, Elizondo G, Wittenberg J, Lee AS, Josephson L, Brady TJ. Ultrasmall superparamagnetic iron oxide: an intravenous contrast agent for assessing lymph nodes with MR imaging. *Radiology* 1990;175:494–498